

## Article

# Towards Photothermal Acid Catalysts Using Eco-Sustainable Sulfonated Carbon Nanoparticles—Part II: Thermal and Photothermal Catalysis of Biodiesel Synthesis

María Paula Militello , Luciano Tamborini , Diego F. Acevedo  and Cesar A. Barbero \* 

Research Institute for Energy Technologies and Advanced Materials (IITEMA), National University of Río Cuarto (UNRC)-National Council of Scientific and Technical Research (CONICET), Río Cuarto 5800, Argentina; mmilitello@exa.unrc.edu.ar (M.P.M.); ltamborini@exa.unrc.edu.ar (L.T.); dacevedo@ing.unrc.edu.ar (D.F.A.)

\* Correspondence: cesarbarbero@gmail.com or cbarbero@exa.unrc.edu.ar; Tel.: +54-3584028768

**Abstract:** The main goal of this work is to evaluate the ability of sulfonated carbon nanoparticles (SCNs) to induce photothermal catalysis of the biodiesel synthesis reaction (transesterification of natural triglycerides (TGs) with alcohols). Carbon nanoparticles (CNs) are produced by the carbonization of cross-linked resin nanoparticles (RNs). The RNs are produced by condensation of a phenol (resorcinol or natural tannin) with formaldehyde under ammonia catalysis (Stober method). The method produces nanoparticles, which are carbonized into carbon nanoparticles (CNs). The illumination of CNs increases the temperature proportionally (linear) to the nanoparticle concentration and exposure time (with saturation). Solid acid catalysts are made by heating in concentrated sulfuric acid (SEAr sulfonation). The application of either light or a catalyst (SCNs) (at 25 °C) induced low conversions (<10%) for the esterification reaction of acetic acid with bioethanol. In contrast, the illumination of the reaction medium containing SCNs induced high conversions (>75%). In the case of biodiesel synthesis (transesterification of sunflower oil with bioethanol), conversions greater than 40% were observed only when light and the catalyst (SCNs) were applied simultaneously. Therefore, it is possible to use sulfonated carbon nanoparticles as photothermally activated catalysts for Fischer esterification and triglyceride transesterification (biodiesel synthesis).

**Keywords:** nanoparticles; photothermal catalysis; biodiesel synthesis; sulfonation; Stober; transesterification; bioethanol; sunflower oil



**Citation:** Militello, M.P.; Tamborini, L.; Acevedo, D.F.; Barbero, C.A. Towards Photothermal Acid Catalysts Using Eco-Sustainable Sulfonated Carbon Nanoparticles—Part II: Thermal and Photothermal Catalysis of Biodiesel Synthesis. *C* **2024**, *10*, 94. <https://doi.org/10.3390/c10040094>

Academic Editors: Sergey Mikhalovsky, Joaquín Silvestre-Albero and Rosa Busquets

Received: 17 September 2024

Revised: 28 October 2024

Accepted: 29 October 2024

Published: 4 November 2024



**Copyright:** © 2024 by the authors. Licensee MDPI, Basel, Switzerland. This article is an open access article distributed under the terms and conditions of the Creative Commons Attribution (CC BY) license (<https://creativecommons.org/licenses/by/4.0/>).

## 1. Introduction

The synthesis of biodiesel involves the transesterification of triglycerides with simple alcohols (methanol or ethanol) [1,2]. The transesterification reaction is slow and must be catalyzed by acidic or basic catalysts [3,4]. Solid catalysts are less corrosive than molecules (e.g., sulfuric acid) and can be separated more easily from the reaction medium [5–7]. Although solid catalysts, such as polymers [8,9] or ceramics [10,11], have been used, catalysts based on carbonaceous materials are preferred due to their chemical stability and low cost [12,13]. While raw carbon materials are able to catalyze the transesterification reaction, due to the presence of acidic (–COOH) groups on the surface [14,15], the catalytic activity is low because the acid groups are weak. To improve catalytic activity, the catalyst surface can be modified by attaching strong acidic (e.g., sulfonic [16]) or basic (e.g., tetrabutylammonium hydroxide) groups [17]. Acid catalysts have been more widely used due to their stability and compatibility with fats containing free fatty acids [18,19]. Therefore, sulfonated carbon nanoparticles could act as catalysts in biodiesel synthesis (transesterification of natural triglycerides) even in the presence of free fatty acids. The incorporation of sulfonic (–SO<sub>3</sub>H) groups on a carbon surface can be achieved by electrophilic aromatic substitution on the aromatic rings of the graphenic planes (edges) [20–24].

Carbonaceous materials absorb light in a wide range of wavelengths (from ultraviolet to far infrared) [25,26], allowing the nanocatalyst to be heated by white light [27–29]. In this way, photothermal catalysis with solar energy can be implemented. The vast majority of carbon-based catalysts use massive, highly porous materials (e.g., activated carbon), which have large surface areas ( $>1000 \text{ m}^2/\text{g}$ ) [30,31]. However, high-surface-area materials contain a high proportion of micropores ( $d < 2 \text{ nm}$ ) that are difficult to access by molecules in solution [32,33]. On the other hand, carbon nanospheres have smaller surface areas (which also depends on their concentration in the solution), but access by the reactants to the catalytic surface is only controlled by mass transport in the liquid phase [34–36]. For this reason, functionalized carbon nanoparticles (e.g., carbon nanotubes) have been used as catalysts [37,38].

The development of the Stober method to produce carbon nanospheres [39,40] allows for the production of carbon-nanoparticle substrates of catalysts for the synthesis of biodiesel. In a previous work (Part I [41]), the synthesis of the resin nanospheres (resorcinol/formol (RF)) and tannin/formol (TF) using the Stober method is described [41]. The resin nanospheres were pyrolyzed in an inert atmosphere, producing carbon nanospheres. Both resin and carbon nanospheres were characterized using DLS, SEM, TEM, and  $\text{N}_2$  adsorption isotherms [41]. They were subsequently sulfonated with concentrated sulfuric acid at various temperatures. The modification degree was measured by EDX, TGA, and acid–base return titration. The nanospheres showed catalytic activity that was equal to or better than conventional solid catalysts during thermal Fischer esterification [41]. Since the reaction mechanisms of Fischer esterification and transesterification are quite similar [42,43], sulfonated carbon nanospheres can be used as catalysts in biodiesels synthesis (transesterification of natural triglycerides).

In this work, the photothermal properties of carbon spheres are evaluated. Then, the material's performance in the thermal catalysis of biodiesel (transesterification of natural triglycerides) is measured. Subsequently, photothermally activated catalysis of the Fischer esterification and synthesis of biodiesel (transesterification) is studied.

## 2. Materials and Methods

### 2.1. Fabrication of Sulfonated Carbon Nanoparticles

The synthesis of sulfonated carbon nanoparticles was performed as described in Part I [1].

#### 2.1.1. Resin Nanoparticles

The synthesis of the resin nanoparticles was conducted using two types of organic precursor pairs: resorcinol (98%, Fluka, Buch, Switzerland) or wood (breakax, *Schinopsis lorentzii*) tannin (Fabriquimica, Buenos Aires, Argentina) and formaldehyde (37%, Cicarelli, San Lorenzo, Argentina). In the Stober synthesis, ammonia solution (25%, Cicarelli, San Lorenzo, Argentina) was used as the catalyst. The solvent was a mixture of double-distilled water (W) and ethanol (EtOH) (96% *v/v*, Porta, Cordoba, Argentina). For all syntheses, the EtOH/W volumetric ratio used was 0.393, and the catalyst concentration was 0.0529 M. The mole ratio of aldehyde to resorcinol (A/P) was 2:1 for the RF resins, while the ratio of the tannin (P) mass to formaldehyde solution was 0.475 g/mL. Only the mass ratio of resorcinol (or tannin) to catalyst was varied. The resin nanoparticles were named RF-x (resorcinol) or TF-x (tannin), where x is the ratio, in mass, of the phenolic precursor to catalyst. The reaction mixture was placed in a closed glass flask and magnetically stirred for 24 h at 30 °C. Then, the flask was placed in an autoclave and heated at 100 °C for 24 h. The resin nanoparticles were centrifuged to separate them. Then, they were thoroughly washed with distilled water and dried in an oven for 48 h at 100 °C [41].

#### 2.1.2. Carbonization of Resin Nanoparticles

The resin nanoparticles obtained with Stöber's methods were pyrolyzed to produce carbon nanoparticles. To do that, the samples were heated at a rate of 1 °C/min up to

350 °C, then maintained at 350 °C for 2 h, heated at 1 °C/min up to 600 °C, followed by an isothermal period of 4 h at 600 °C. The obtained carbon nanospheres were named CRF-x/600 (resorcinol phenolic precursor) and CTF-x/600 (tannin phenolic precursor). The heating rate is larger than that used in bulk resins, since the small size of the nanoparticles allows the pyrolysis gasses to escape the resin mass without breakage.

### 2.1.3. Sulfonation of Resin and Carbon Nanoparticles

This sulfonation functionalization method consists of heating the nanoparticles in concentrated sulfuric acid [44,45]. In total, 2 g of resin or carbon nanoparticles was dispersed (ultrasound) in 100 mL of concentrated H<sub>2</sub>SO<sub>4</sub> (98%, Merck, Darmstadt, Germany). The dispersion of resin nanoparticles was heated for 15 min at 50 °C, while the carbon nanoparticles were heated for 60 min at 80 °C. The difference is due to the higher reactivity of the resin mass (compared to carbon), which causes unnecessarily higher temperatures or longer reaction times. Moreover, the resin ether linkages could be hydrolyzed during a harsher treatment. The dispersion was then poured onto 100 g of ice to dilute the acid and quench the reaction. The sulfonated particles were separated by centrifugation, washed thoroughly with distilled water and dried at 100 °C for 48 h. The sulfonated nanoparticles were named RF-x/H<sub>2</sub>SO<sub>4</sub>/50 (resin) and CRF-x/Tp/H<sub>2</sub>SO<sub>4</sub>/80 (carbon), with resorcinol used as phenolic precursor, and TF-x/H<sub>2</sub>SO<sub>4</sub>/50 and CTF-x/Tp/H<sub>2</sub>SO<sub>4</sub>/80 when tannin-based materials were used. In the names, Tp refers to the pyrolysis temperature.

### 2.2. Measurement of Photothermal Effects

Radiation absorption measurements were carried out on CRF-x/600 carbon nanoparticles using light (sodium lamp). To carry out the measurements, carbon nanoparticles were dispersed in water, on the one hand, and on the other, in methanol, at different concentrations (0, 0.1, 0.2, 0.3, 0.4 and 0.5% *w/v*). The total volume of each sample was 1 mL. These were placed in tubes of polymeric material transparent to radiation. The experiments consisted of irradiating the samples with the laser and carrying out temperature measurements of the suspensions at regular time intervals. The illumination of the tubes was carried out from the bottom of the tubes, and the temperature measurement was carried out with an infrared thermometer (TES-1327K).

### 2.3. Transesterification of Sunflower Oil

Biodiesel synthesis was carried out by transesterification reactions of sunflower oil (Natura<sup>®</sup>, Gral Deheza, Cordoba, Argentina) with dried (<0.5% water) bioethanol (99.5%, Bio4, Rio Cuarto, Argentina). The reactions were carried out in a 250 mL flask, partially immersed in a glycerin heating bath, at reflux, and with magnetic stirring. The molar ratio of oil to alcohol, temperature, reaction time, and amount of catalyst were varied between experiments in order to analyze the influence of these variables on the conversion. In that way, optimal reaction conditions are found and then applied in photothermal catalysis studies. After the reaction time in each of the experiments had finished, the reaction mixture was transferred to plastic tubes to separate the catalyst from the reaction medium by centrifugation. Subsequently, the supernatant liquid, consisting of two immiscible phases, was transferred to a 250 mL separating bottle to facilitate the recovery of the alkyl-ester-rich phase once the mixture reached room temperature. Normally, the phase at the top of the ampoule is the phase of interest, rich in alkyl esters and of lower density, while the lower phase is rich in glycerol and alcohol. However, the position of the phases can vary according to the conversion achieved, which causes variations in the density of the product phase of interest: when the conversion is very low, the lower phase consists mainly of unreacted sunflower oil and alkyl esters, while the upper phase is basically composed of alcohol. The phase rich in alkyl esters was analyzed using gas chromatography (GC). Its density and volume were previously measured, the data of which are necessary to calculate the mass of the recovered phase and, finally, the reaction yield.

### 3. Results and Discussion

First, the photothermal properties of the carbon nanoparticles were studied. The data were measured using the CRF-6/600 sulfonated carbon nanoparticles. The relevant data [41] of those nanoparticles are described in Table 1.

**Table 1.** Physicochemical parameters of carbon nanoparticles (CRF-6/600).

Nd (nm)	S <sub>BET</sub> (m <sup>2</sup> /g)	Vt (cm <sup>3</sup> /g)	Dp (nm)
590	8.27	0.058	2.6

Where Nd is the particle diameter (measured by DLS), S<sub>BET</sub> is the specific surface area, Vt is the total pore volume (both measured from N<sub>2</sub> isothermal data), Dp is the pore diameter (calculated by DFT from fitting the N<sub>2</sub> isotherm data), and ngs is the specific number of sulfonic acid groups (measured by return titration).

#### 3.1. Photothermochemistry of Carbon Nanoparticles

Light absorption tests were carried out on the synthesized carbon materials, dispersed in different media (water and methanol). The objective of these experiences was to evaluate the feasibility of raising the temperature of the particles dispersion by means of irradiation. The measurements were carried out with dispersions of CRF-6/600 non-functionalized carbon particles (Figure 1).

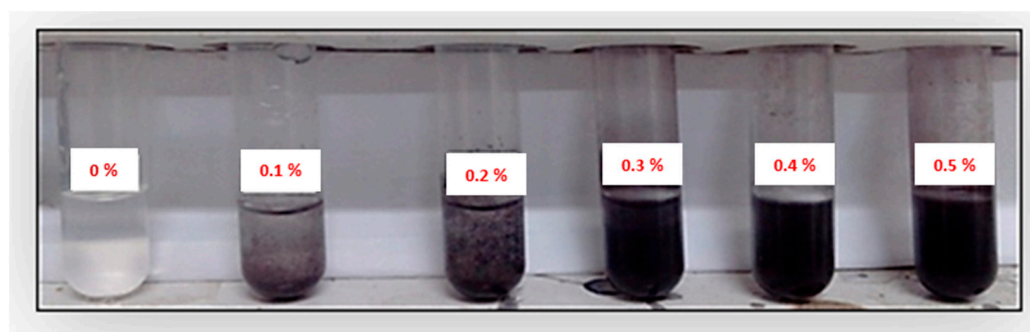


**Figure 1.** Photographs of carbon nanoparticle (CRF-6/600) dispersions in water at different concentrations (% *p/v*). Volume = 1 mL.

The colloidal dispersions are stable for days, likely due to the charges present in the spontaneously oxidized carbon surface of the nanoparticles. The photothermal measurements were made as described in the experimental part. The data collected during the experiments were temperature values of the medium in which the particles are suspended, as a function of time and concentration. These were taken in triplicate and average values were calculated. The results obtained for suspensions in water are graphed in Figure 2, while those corresponding to dispersions in ethanol are shown in Figure 3.

The temperature increases with irradiation time (Figures 2A and 3A), likely due to the fact that the heat generated by light absorption is dissipated faster to the surroundings at higher temperatures, according to Newton's law. On the other hand, there is a linear dependence of the temperature with respect to the concentration of nanoparticles in the dispersions for a given irradiation time, obeying a relationship related to Lambert–Beer law. This is noteworthy as it implies that the light traverses the whole volume without complete extinction. That is, all the nanoparticles in the light path absorb light, even for the highest concentration (0.5%). Otherwise, only part of the dispersion will be affected, and most of the catalyst will be unused. In the case of a 0.5% *w/v* dispersion in water, the temperature increase is 2 times higher than that seen in the pure solvent (Figure 2B). The temperature increase experienced by a dispersion in methanol whose carbon concentration is 0.5% *w/v* is 4 times larger than the increase experienced in the absence of carbon nanoparticles (Figure 3B). In this way, the ability of coal particles to absorb near-infrared radiation is shown.

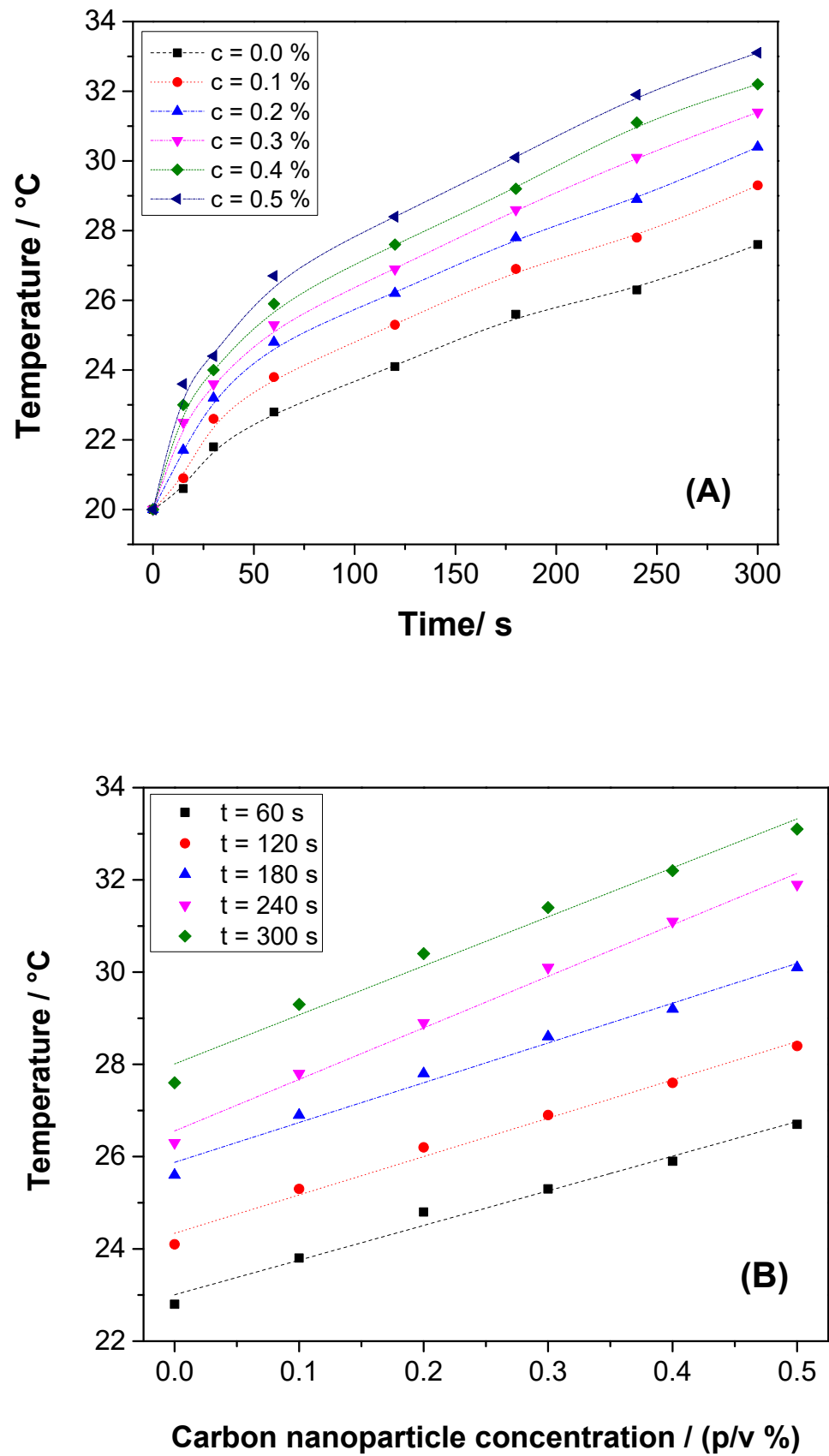


**Figure 2.** Dependence of temperature on time (A) and concentration (B) of CRF-6/600 in dispersions in water irradiated with NIR laser—laser power: 100 mW;  $\lambda = 780$  nm; volume of dispersions = 1 mL.

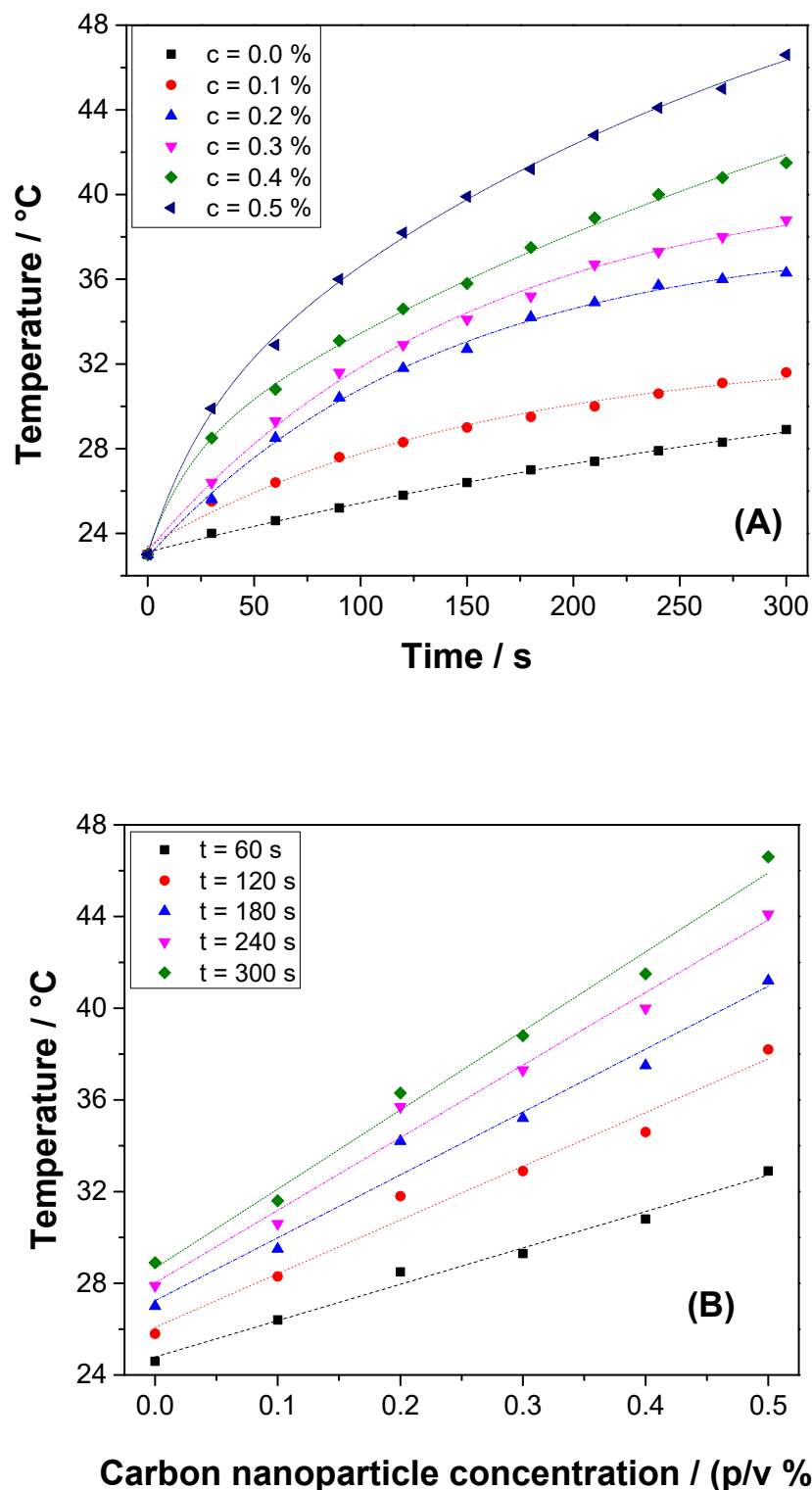


**Figure 3.** Dependence of temperature on time (A) and concentration of (B) CRF-6/600 in dispersions in ethanol irradiated with NIR laser—laser power: 100 mW;  $\lambda = 780$  nm; volume of dispersions = 1 mL.

As seen in Figure 4, the temperature changes in methanol and water increase linearly with concentration, but the slope is lower due to the greater specific heat capacity of water (4.186 J/g $^{\circ}$ K) compared to methanol (2.460 J/g $^{\circ}$ K). Light absorption produces a similar amount of heat in the carbon nanoparticles, which induces a thermal change inversely proportional to the specific heat capacity.

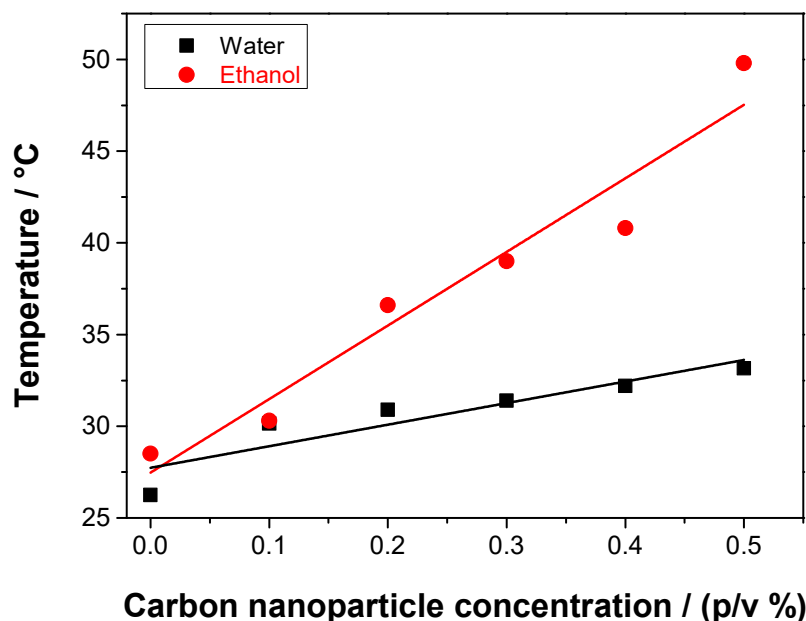
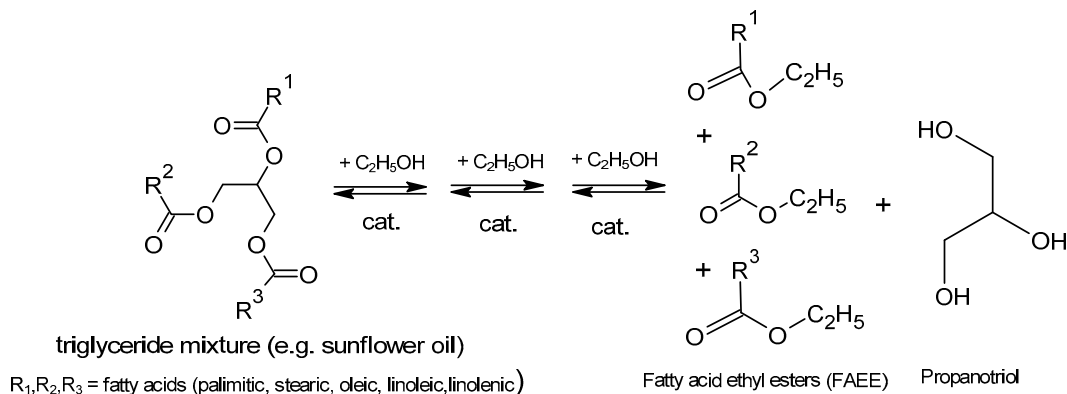


**Figure 4.** Temperature dependence on the concentration of CRF-6/600, dispersed in methanol and water—volume = 1 mL; irradiation time = 30 s.

### 3.2. Thermal Catalysis of Sunflower Oil Transesterification

The synthesis of biodiesel from natural oils or fats (e.g., sunflower oil) involves the trans-esterification of triglycerides with alcohols (e.g., bioethanol) under catalysis (Scheme 1).



**Scheme 1.** Trans-esterification reaction of sunflower oil with bioethanol.

As can be seen (Scheme 1), the reaction occurs in three consecutive steps, and each one requires catalysis. Moreover, all reactions are reversible. To obtain a high conversion, the equilibria should be displaced to products. This is achieved by adding an excess of the alcohol (bioethanol).

The catalytic activity of the sulfonated carbon nanoparticles toward the trans-esterification reactions of sunflower oil with ethanol was studied. Various reactions were carried out, in which parameters such as temperature, oil/alcohol ratio, reaction time, and percentage of added catalyst were varied. The reaction products were analyzed using gas chromatography. The effect of different parameters (temperature, time, amount of catalyst, oil/alcohol ratio) in the thermal conversion of triglycerides and bioethanol to ethyl esters and glycerol while being catalyzed by sulfonated carbon nanoparticles are analyzed. The sulfonated carbon nanoparticles used were CRF-6/600/H<sub>2</sub>SO<sub>4</sub>/80. The relevant data [41] of those nanoparticles are described in Table 2.

**Table 2.** Physicochemical parameters of carbon nanoparticles (CRF-6/600/H<sub>2</sub>SO<sub>4</sub>/80).

Nd (nm)	S <sub>BET</sub> (m <sup>2</sup> /g)	Vt (cm <sup>3</sup> /g)	Dp (nm)	ngs (nmoles/g)
590	8.27	0.058	2.6	8.99

Where Nd is the particle diameter (measured by DLS), S<sub>BET</sub> is the specific surface area, Vt is the total pore volume (both measured from N<sub>2</sub> isothermal data), Dp is the pore diameter (calculated by DFT from fitting the N<sub>2</sub> isotherm data), and ngs is the specific number of sulfonic acid groups (measured by return titration).

### 3.2.1. Effect of the Amount of Catalyst

To study the effect that the amount of added catalyst has on the yield of the transesterification reaction of sunflower oil with EtOH, the catalyst amount was varied, maintaining the other parameters constant. The results obtained through these experiences are shown in Table 3.

**Table 3.** Yields of ethyl esters obtained for transesterification reactions of sunflower oil with ethanol at different percentages of catalyst—catalyst used: CRF 6/600/H<sub>2</sub>SO<sub>4</sub>/80; oil/alcohol molar ratio: 1:20.

% Catalyst	t (h)	T (°C)	Oil Mass (g)	FAEE Mass (g)	% FAEE <sub>masa</sub>	% FAEE <sub>mol</sub>
3	5	90	10	0	0	0
5	5	90	10	6.186	61.86	57.01
7.5	5	90	10	7.825	78.25	72.01
10	5	90	10	8.224	82.24	75.79

As seen in Table 3, when 3% of catalyst was used, there was no appreciable conversion, since the characteristic peaks did not appear in the chromatogram of either of the two product phases.

The components of the rest of the ethyl ester mixtures were identified and quantified using gas chromatography. The individual conversion of each ester was calculated. The values obtained are shown in Table 4.

**Table 4.** Effect of the percentage of catalyst on the composition of the product and the individual yield of fatty acids ethyl esters (FAEEs) in the trans-esterification reaction of sunflower oil with ethanol—catalyst used: CRF 6/600/H<sub>2</sub>SO<sub>4</sub>/80; oil/alcohol molar ratio: 1:20; temperature: 90 °C; reaction time: 5 h.

% Catalyst =	5%	7.50%	10%
Fatty Acid	% FAEE		
Palmitic	9.52	9.61	9.73
Linoleic	52.29	30.85	50
Oleic	34.12	53.59	36.47
Stearic	4.06	5.95	3.81

The results indicate that by adding low amount of catalyst, fewer available active sites are available, which causes low biodiesel yield. From Table 4, it can be stated that, in all the cases studied, the conversions of oleic and palmitic acids to oleate and palmitate, respectively, are the highest. In the case of palmitate, this would be related to the lower molecular weight of the acid, which has a shorter carbon chain than the rest of the acids that make up the oil (16 carbons versus 18 carbons for oleic, linoleic, and stearic acids). Indeed, using 10% catalyst, it is possible to convert 100% of the palmitic acid present in the oil to ethyl palmitate.

### 3.2.2. Effect of Reaction Temperature

In order to analyze the effect that temperature has on the yield of the transesterification reaction of sunflower oil with EtOH, the values of the oil/alcohol molar ratio (1:20), stirring speed (1300 rpm), reaction time (5 h) and optimum amount of catalyst added (10% w/w

with respect to the mass of oil). The amount of initial sunflower oil was kept fixed at 10 g, the volume of ethanol at 13.2 mL, and the temperature was varied. Experiments were carried out at 60, 75, and 90 °C. The catalyst used for the experiment was CRF 6/600/H<sub>2</sub>SO<sub>4</sub>/80. The results obtained are summarized in Table 5.

**Table 5.** Yields of ethyl esters obtained for transesterification reactions of sunflower oil with ethanol at different temperatures. Catalyst used: CRF 6/600/H<sub>2</sub>SO<sub>4</sub>/80; mass percentage of catalyst with respect to oil: 10%; oil/alcohol molar ratio: 1:20; reaction time: 5 h.

T (°C)	% Catalyst	Time (h)	Oil Mass (g)	FAEE Mass (g)	% FAEE <sub>masa</sub>	% FAEE <sub>mol</sub>
60	10	5	10	0.150	1.5	1.38
75	10	5	10	0.774	7.74	7.13
90	10	5	10	8.224	82.24	75.79

The composition of the mixtures of ethyl esters, which were the product of the transesterification reactions with EtOH, was analyzed and quantified using gas chromatography, and the results obtained are expressed in Table 6.

**Table 6.** Effect of the reaction temperature on the composition of the product and the individual yield of fatty acids ethyl esters (FAEEs) in the transesterification reaction of sunflower oil with ethanol. Catalyst used: CRF 6/600/H<sub>2</sub>SO<sub>4</sub>/80; mass percentage of catalyst with respect to oil: 10%; oil/alcohol molar ratio: 1:20; reaction time: 5 h.

Temperature (°C) =	60	75	90
Fatty Acid	% FAEE in the Mixture		
Palmitic	6.69	8.32	9.73
Linoleic	34.31	49.01	50
Oleic	56.39	39.19	36.47
Stearic	2.61	3.47	3.81

From Tables 5 and 6, it can be concluded that the individual conversions of each component increase with increasing temperature; the overall conversion exhibits an exponential growth with increasing temperature, in agreement with the Arrhenius equation (Figure 5). It follows, then, that the catalyst does not present diffusion problems and that, by increasing the temperature, the reaction rate can be increased. It would also indicate that the functional groups responsible for catalysis are found mostly on the surface.

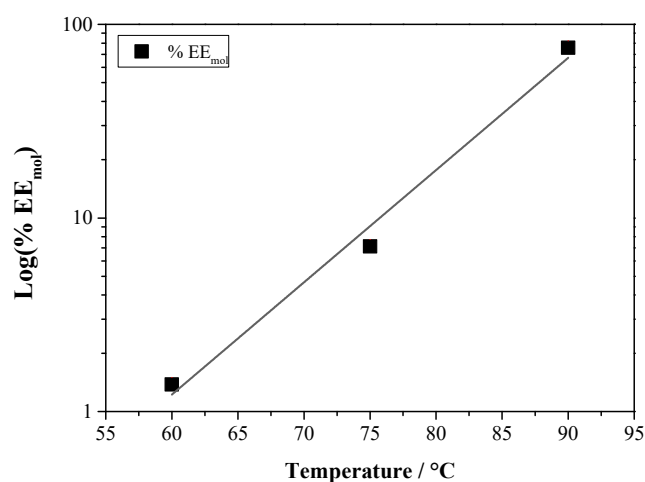


**Figure 5.** Dependence of the yield of fatty acid ethyl esters on the reaction temperature (Arrhenius plot) in the transesterification of sunflower oil with ethanol. Catalyst used: CRF 6/600/H<sub>2</sub>SO<sub>4</sub>/80; mass percentage of catalyst with respect to oil: 10%; oil/alcohol molar ratio: 1:20; reaction time: 5 h.

### 3.2.3. Effect of Reaction Time

For the analysis of the effect that the reaction time has on the yield of the transesterification reaction of sunflower oil with EtOH, a series of experiences were carried out, among which the values of the molar ratio oil/alcohol (1:20), stirring speed (1300 rpm), reaction temperature (90 °C), and amount of added catalyst (10% *w/w* with respect to the mass of oil) were kept fixed. The amount of oil added at the beginning of the reaction was 10 g in all cases, the volume of ethanol was 13.2 mL, and the reaction time was varied between 2.5 and 7.5 h. The catalyst used to analyze this effect was CRF 6/600/H<sub>2</sub>SO<sub>4</sub>/80. The yields of ethyl esters obtained from these experiments are shown in Table 7.

**Table 7.** Yields of fatty acid ethyl esters (FAEEs) obtained for transesterification reactions of sunflower oil with ethanol at different reaction times. Catalyst used: CRF 6/600/H<sub>2</sub>SO<sub>4</sub>/80; temperature: 90 °C; mass percentage of catalyst with respect to oil: 10%; oil/alcohol molar ratio: 1:20.

Time (h)	% Catalyst	T (°C)	Oil Mass (g)	FAEE Mass (g)	% FAEE <sub>masa</sub>	% FAEE <sub>mol</sub>
2.5	10	90	10	1.681	16.81	15.47
5	10	90	10	8.224	82.24	75.79
7.5	10	90	10	8.321	83.21	76.53

Table 7 shows that the yield of the reaction is increasing throughout the time range evaluated. However, after 5 h of reaction and up to 7.5 h, the difference in yield is only 1%; beyond this time, the energy expenditure invested in the reaction is not compensated by the benefit obtained as a result of an increase in yield. The composition of the mixtures of the esters produced during the experiments and the individual conversion percentage of fatty acids, determined using gas chromatography, are shown in Table 8.

**Table 8.** Effect of reaction time on product composition and individual yield of fatty acids ethyl esters (FAEEs) in the transesterification of sunflower oil with ethanol. C atalyst used: CRF 6/600/H<sub>2</sub>SO<sub>4</sub>/80; temperature: 90 °C; mass percentage of catalyst with respect to oil: 10%; oil/alcohol molar ratio: 1:20.

Time (h) =	2.5	5	7.5
Fatty Acid	% FAEE		
Palmitic	8.43	9.73	7.93
Linoleic	48.7	50	45.16
Oleic	38.59	36.47	43.26
Stearic	4.28	3.81	3.64

As can be seen, the yield of the individual esters increases with the reaction time.

### 3.2.4. Effect of Oil/Alcohol Ratio

For the analysis of the influence of the oil/alcohol molar ratio on the yield of the transesterification reaction of sunflower oil with EtOH, various experiments were carried out under the following conditions: stirring speed values remained fixed (1300 rpm), temperature (90 °C), amount of catalyst (10% *w/w* with respect to the mass of oil), and reaction time (5 h). The mass of vegetable oil in each experience was 10 g. The oil/alcohol ratio was varied, using three molar ratios: 1:5, 1:12, and 1:20. The catalyst used for the study of this variable was CRF 6/600/H<sub>2</sub>SO<sub>4</sub>/80. The results obtained from the analysis of the products by GC are shown in Table 9.

From the analysis of the values tabulated in Table 9, it was found that the conversion reaches a maximum, in the evaluated range, when the amount of alcohol added is greater (oil/alcohol molar ratio equal to 1:20). Based on this observation, it was determined to carry out subsequent experiments with this ratio of reagents, in order to have an acceptable performance, without wasting large volumes of ethanol, a necessary condition for a poten-

tial application on an industrial scale. The compositions of the mixtures of FAEs, obtained using gas chromatography, are shown in Table 10.

**Table 9.** Yields of ethyl esters obtained for transesterification reactions of sunflower oil with ethanol, using different triglycerides/ethanol ratios. Catalyst used: CRF 6/600/H<sub>2</sub>SO<sub>4</sub>/80; temperature: 90 °C; mass percentage of catalyst with respect to oil: 10%; reaction time: 5 h.

Triglycerides/Ethanol	FAEE Mass (g)	% EE <sub>masa</sub>	%EE <sub>mol</sub>
1:05	4.601	46.01	42.22
1:12	6.299	62.99	58.12
1:20	8.224	82.24	75.79

**Table 10.** Effect of the triglycerides/alcohol ratio on the composition of the product and the individual yield of fatty acids in fatty acid ethyl esters (FAEEs) in the transesterification of sunflower oil with ethanol. Catalyst used: CRF 6/600/H<sub>2</sub>SO<sub>4</sub>/80; temperature: 90 °C; mass percentage of catalyst with respect to oil: 10%; reaction time: 5 h.

Triglycerides/Ethanol Ratio	1:05	1:12	1:20
<b>Fatty Acid</b>	<b>% FAEE</b>		
Palmitic	9.92	5.09	9.73
Linoleic	57.15	48.16	50
Oleic	28.98	43.48	36.47
Stearic	3.95	3.27	3.81

The dependence that exists between the variables, molar ratio, and yield is linear, as shown in the graph of Figure 6.

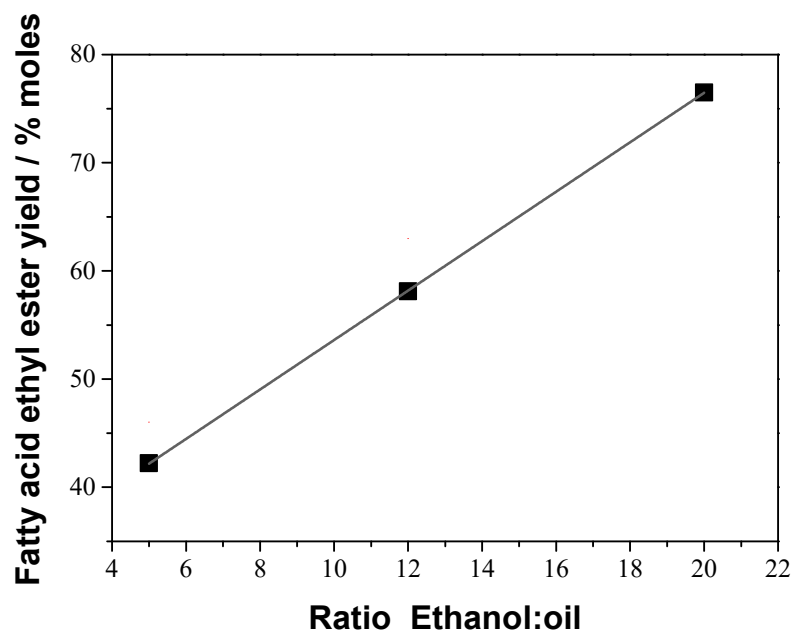


**Figure 6.** Dependence of the yield of ethyl esters with the molar ratio of ethanol/oil reagents in the transesterification of sunflower oil with ethanol. Catalyst used: CRF 6/600/H<sub>2</sub>SO<sub>4</sub>/80; temperature: 90 °C; mass percentage of catalyst with respect to oil: 10%; reaction time: 5 h.

While no cycling experiments were performed with the nanoparticles, the sulfonated carbon and oil chemistry is the same as that used by us [19] before. A loss of 40% activity in 3 cycles was shown. However, such a loss could be due to poisoning by other components of the oil (phospholipids, gums, etc.), which can be removed by washing with detergents, improving the reusability.

### 3.2.5. Optimal Parameters for the Biodiesel Synthesis Reaction

To conclude the study of the effect of the studied variables, the optimal reaction conditions found were established. The conditions for the sunflower oil transesterification reaction with EtOH are detailed in Table 11.

**Table 11.** Optimal reaction conditions for transesterification of sunflower oil with ethanol. Catalyst used: CRF-6/600/H<sub>2</sub>SO<sub>4</sub>/80.

Parameter	Optimal Value
Temperature	90 °C
Reaction time	5 h
Catalyst Percentage	10% <i>w/w</i>
Sunflower oil/methanol ratio	1:20

### 3.2.6. Comparison with Other Sulfonated Catalysts

From the data described above, it can be ascertained that sulfonated carbon nanoparticles (CRF-6/600/H<sub>2</sub>SO<sub>4</sub>/80) are able to catalyze the transesterification reaction of sunflower oil with bioethanol. Since we have synthesized (Part I, Ref. [1]) other sulfonated CRF (with resin made from resorcinol) and CTF (with resin made from tannin) nanoparticles, the catalytic activity is compared (Table 12 and Figure 7). The CTF (tannin)-based catalyst shows lower conversions than the CRF (resorcinol)-based materials. A similar effect was observed for Fischer's esterification of acetic acid with methanol [41].

**Table 12.** Yield in mass (% EE<sub>mass</sub>) and in moles (% EE<sub>mol</sub>) of ethyl esters in transesterification reactions of sunflower oil with ethanol. Reaction conditions: temperature: 90 °C, reaction time: 5 h, catalyst percentage (*w/w* with respect to oil): 10%, oil/alcohol molar ratio: 1:20, magnetic stirring: 1300 rpm, Reflux.

Catalyst	% EE <sub>mass</sub>	% EE <sub>mol</sub>	Label
CRF-6/H <sub>2</sub> SO <sub>4</sub> /80/600	82.24	75.79	CRF-6
CRF-4/H <sub>2</sub> SO <sub>4</sub> /80/600	79.43	73.22	CRF-4
CRF-2/H <sub>2</sub> SO <sub>4</sub> /80/600	81.67	75.21	CRF-2
CTF-1/H <sub>2</sub> SO <sub>4</sub> /80/600	68.85	63.44	CTF-1
CTF-1.5/H <sub>2</sub> SO <sub>4</sub> /80/600	59.78	55.02	CTF-1.5
CTF-6/H <sub>2</sub> SO <sub>4</sub> /80/600	62.33	57.42	CTF-6
Amberlite IR-120	NO CONVERSION		PSS
Nafion 117	NO CONVERSION		Nafion
SBA-15 sulfonada	NO CONVERSION		SBA15-S
SBA-15/RFsulf #	85.44	78.59	SBA-15-RF-S

# Reaction time equal to 8 h.

On the one hand, solid acid catalysts based on polymers (Nafion 117 and Amberlite IR-120) or silica (sulfonated SBA-15) [46] do not show any conversion (Table 12 and Figure 7). On the other hand, such materials show catalysis of the Fischer's esterification reaction [41], suggesting that the hydrophobic nature of the carbon substrate allows for the interaction of the acidic sites with the triglycerides. Accordingly, a silica material decorated with RF carbon (sulfonated SBA-15/RF) shows the largest conversion (Table 12 and Figure 7), indicating the key role of carbon in the catalysis of the transesterification reaction. The partial hydrophobicity of the added RF carbon (SBA 15-RF) impregnating the walls of the mesoporous silica allows for wetting by the solution and makes the material a good catalyst of the transesterification of triglycerides with ethanol (Figure 7).

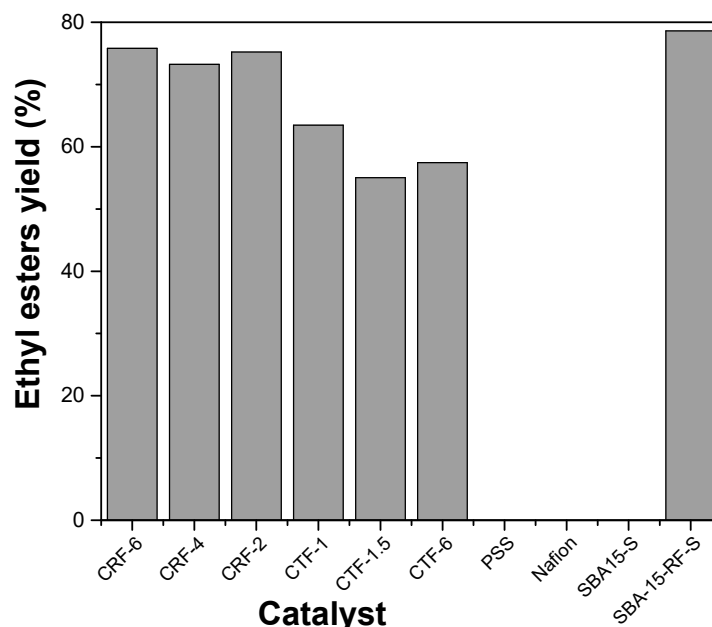


**Figure 7.** Comparison of the transesterification yield using sulfonated carbon nanoparticles (produced from RF and TF resin nanoparticles) with commercial (Amberlite<sup>®</sup> and Nafion<sup>®</sup>) materials and sulfonated mesoporous silica (SBA15-S and SBA15-RF-S) [46].

### 3.3. Photothermal Catalysis

First, the photothermal catalysis of the Fischer esterification reaction is tested for the acetic acid system with bioethanol.

#### 3.3.1. Photothermal Catalysis of the Fischer Esterification of Acetic Acid with Bioethanol

The feasibility of catalyzing the Fischer esterification reaction, using radiation in the visible spectrum as an energy source, was analyzed using a reagent system consisting of acetic acid and bioethanol. The results obtained for the material CRF-6/600/H<sub>2</sub>SO<sub>4</sub>/80 are represented in Figure 8. From these results, it can be seen that the effect of irradiation, in the absence of a catalyst, on the progress of the reaction is just 1.3%. This arises from comparing the conversion achieved in the absence of a catalyst for an illuminated system (+hν, −Cat, 8.36% conversion) and another in the dark (−hν, −Cat, 7.05% conversion). Thus, the thermal effect of heating the medium by the mere presence of the lamp is low. On the other hand, the presence of the sulfonated carbon nanoparticles shows a catalytic effect of 5.7% in conversion (−hν, +Cat, 12.79% conversion vs. −hν, −Cat, 7.05% conversion). Even at low temperatures, the catalyst increases the esterification rate. Finally, when both conditions are applied to the reaction system (+hν, +Cat), the photothermal heating of the active surface of the catalyst indicates an increase of ca. 6 times in the conversion (76.74%), with respect to the thermal catalysis at lower temperatures. The overall effect, compared with the neither catalyzed nor photothermally heated condition, is of ca. 10 times.

It should be noted that, in the experiences in which the cells were illuminated, the bulk solution never exceeded 45 °C, a temperature at which the esterification reaction still presents very low kinetics, and according to the extrapolation of the Arrhenius plot (Figure 5), the yield of FAEEs at 45% is below 1%. These data suggest that the surface temperature of the carbon nanoparticles reaches levels much higher than that of the bulk solution and that heating due to the effect of light is located on their surface. Moreover, the experiment is carried out under continuous illumination. Since the thermal transfer of liquids is slow, higher temperatures can be reached under pulses of high power lasers, as has been shown with Ag nanoparticles [47]. The feasibility of photothermal catalysis using sulfonated carbon nanoparticles in reactions catalyzed by acids is demonstrated.

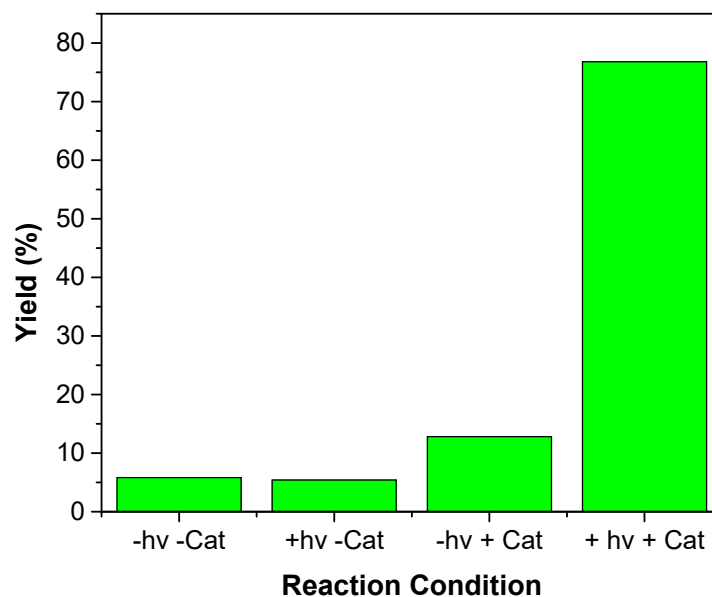


**Figure 8.** Demonstration of the effect of photothermal catalysis on esterification: 0.1% *w/v* of CRF 6/600/H<sub>2</sub>SO<sub>4</sub>/80 as catalyst—acetic acid/ethanol volumetric ratio = 2. Source: sodium vapor lamp ( $\lambda = 589$  nm, power = 525 W/m<sup>2</sup>, distance from source = 40 cm). Irradiation time = 25 min.

### 3.3.2. Photothermal Catalysis of the Transesterification of Sunflower Oil with Ethanol

Using the methodology described in the experimental Section, the possibility of catalyzing the sunflower oil transesterification reaction using radiation in the visible spectrum as an energy source was analyzed. The catalyst used to carry out the tests was CRF-6/600/H<sub>2</sub>SO<sub>4</sub>/80. The results of the experiments, carried out for different reaction times, are summarized in Figure 9.

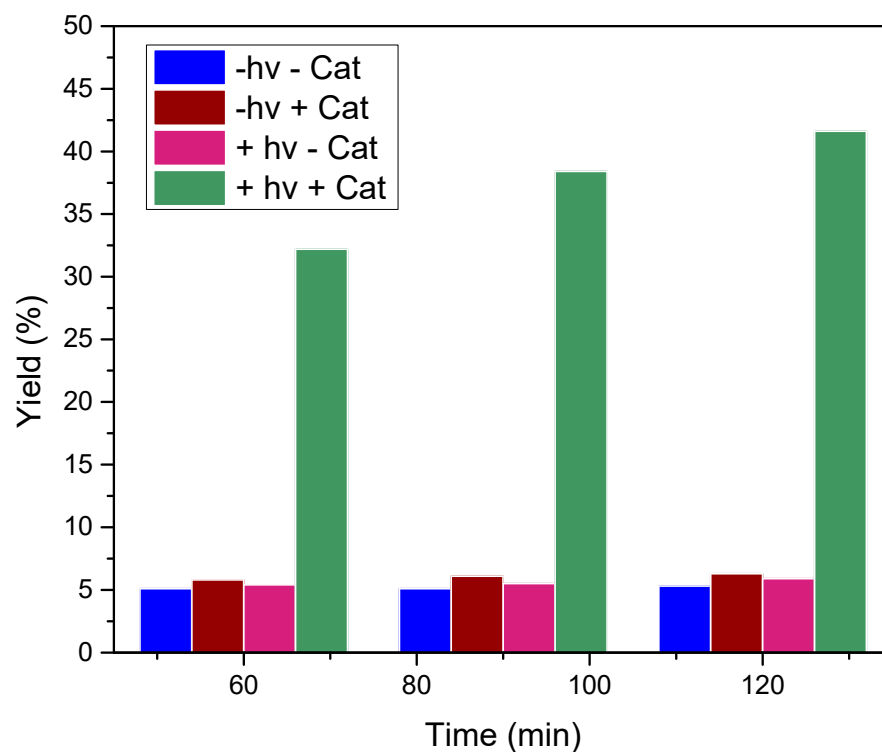


**Figure 9.** Demonstration of the effect of photothermal catalysis in transesterification: 10% *w/w* with respect to sunflower oil of CRF-6/600/H<sub>2</sub>SO<sub>4</sub>/80 as catalyst—oil/EtOH molar ratio = 1:20. Source: sodium vapor lamp ( $\lambda = 589$  nm, power = 525 W/m<sup>2</sup>, distance from the source = 40 cm).

As can be seen (Figure 9), the conversion increases significantly when both light and the catalyst are applied. Moreover, increasing the reaction time increases the % of conversion, suggesting a kinetic effect. On the other hand, the overall conversion is lower than the one observed using sulfonated carbon nanoparticles as thermal catalysts (for 5 h). The complexity (three successive steps) of transesterification, compared with esterification, likely accounts for the difference. In any case, the results suggest that photothermal catalysis of the biodiesel synthesis (transesterification of triglycerides with ethanol) is possible. It should be noted that modified carbon materials are the only solid acid catalyst which combine photothermal heating with acid catalysis. Moreover, while carbon nanoparticles can be used, the application of monolithic porous carbon is not feasible.

#### 4. Conclusions

Phenol–formol resin nanoparticles, made by Stober’s method from phenols (resorcinol, tannin) and formaldehyde, can be carbonized to form carbon nanoparticles. It is possible to photothermally heat the dispersion of carbon nanoparticles in water and methanol. The temperature obtained is higher in methanol due to its lower heat capacity. The carbon nanoparticles can be sulfonated with sulfuric acid (concentrate). It is observed that sulfonated carbon nanoparticles (SCNs) are able to catalyze the transesterification of triglycerides (sunflower oil) with bioethanol (<0.5% water), observing different efficiency for the fatty acids present in the oil. The effect of catalyst amount, triglycerides/ethanol ratio, and reaction time were evaluated. SCN catalysts show different conversion yields. Those made by pyrolysis of resorcinol/formaldehyde nanoparticles (CRF) show larger conversions than those made by carbonization using tannin/formaldehyde resin nanoparticles. Moreover, non-carbon catalysts (Nafion<sup>®</sup>, Amberlite and sulfonated SBA-15) show no conversion for the transesterification reaction. On the other hand, SBA-15 decorated with sulfonated carbon [46] show a high conversion. On the other hand, it was previously observed that SCNs (CRF and CTF) are able to catalyze the esterification of acetic acid with methanol [41], but Nafion<sup>®</sup> and Amberlite<sup>®</sup> catalysts show smaller conversions but are able to catalyze the reaction. It seems that the hydrophobic surface of the carbon is required to interact with the triglyceride molecules, allowing them to reach the acidic catalytic centers, while the same effect is not observed with less hydrophobic acetic acid [41].

Moreover, the effect of temperature is measured to elucidate the photothermal effects on the reaction. It is observed that the application of light or catalysts (SCNs) at 25 °C produces low conversions (<10%) within 2 h. On the contrary, the application of light and catalyst allows for reaching high conversions (>75%). The reaction medium is only heated to ca. 45 °C, suggesting that it is the local photothermal heating of the catalyst (SCNs) at larger temperatures which is responsible for the photothermal activation effect.

The results confirm that photothermal catalysis of acid-catalyzed reactions using SCNs is possible. A similar behavior is observed with the transesterification of triglycerides (sunflower oil) with bioethanol. The application of light to the catalyst-containing reaction medium (SCNs) increases the reaction rate, reaching conversions of ca. 40% after 2 h. The lower degree of final conversion in transesterification (compared to esterification) is probably caused by the complexity of the reaction (three successive transesterification steps per triglyceride molecule).

The results suggest that photothermal catalysis, using sulfonated carbon nanoparticles, is a useful process for biodiesel synthesis and could be applied using sunlight.

**Author Contributions:** Conceptualization, C.A.B. and D.F.A.; methodology, M.P.M. and L.T.; formal analysis, M.P.M., C.A.B. and D.F.A.; investigation, M.P.M. and C.A.B.; resources, C.A.B.; data curation, C.A.B.; writing—original draft preparation, M.P.M. and C.A.B., writing—review and editing, C.A.B.; supervision, D.F.A. and C.A.B., project administration, C.A.B.; funding acquisition, C.A.B. All authors have read and agreed to the published version of the manuscript.

**Funding:** This research was funded by FONCYT (PICT 2450/2019 and PICT II 6/2021), CONICET (PUE of IITEMA) and SECYT-UNRC (PICT SSPR).

**Data Availability Statement:** Data are contained within the article.

**Acknowledgments:** C.A.B., D.F.A. and M.P.M. are permanent researchers of CONICET.

**Conflicts of Interest:** The authors declare no conflicts of interest.

## References

1. Khan, E.; Ozaltin, K.; Spagnuolo, D.; Bernal-Ballen, A.; Piskunov, M.V.; Di Martino, A. Biodiesel from Rapeseed and Sunflower Oil: Effect of the Transesterification Conditions and Oxidation Stability. *Energies* **2023**, *16*, 657. [\[CrossRef\]](#)
2. Anil, N.; Rao, P.K.; Sarkar, A.; Kubavat, J.; Vadivel, S.; Manwar, N.R.; Paul, B. Advancements in Sustainable Biodiesel Production: A Comprehensive Review of Bio-Waste Derived Catalysts. *Energy Convers. Manag.* **2024**, *318*, 118884. [\[CrossRef\]](#)
3. Shaik, M.R.; Khan, M.; Kumar, J.V.S.; Ashraf, M.; Khan, M.; Kuniyil, M.; Assal, M.E.; Al-Warthan, A.; Siddiqui, M.R.H.; Khan, A.; et al. Nano Nickel-Zirconia: An Effective Catalyst for the Production of Biodiesel from Waste Cooking Oil. *Crystals* **2023**, *13*, 592. [\[CrossRef\]](#)
4. Sarangi, P.K.; Singh, A.K.; Ganachari, S.V.; Pengadeth, D.; Mohanakrishna, G.; Aminabhavi, T.M. Biobased Heterogeneous Renewable Catalysts: Production Technologies, Innovations, Biodiesel Applications and Circular Bioeconomy. *Environ. Res.* **2024**, *261*, 119745. [\[CrossRef\]](#)
5. Faruque, M.O.; Razzak, S.A.; Hossain, M.M. Application of Heterogeneous Catalysts for Biodiesel Production from Microalgal Oil—A Review. *Catalysts* **2020**, *10*, 1025. [\[CrossRef\]](#)
6. Zhang, Y.; Tong, C.; Lv, X.; Lou, S.; Liao, S.; Feng, J.; Liu, L.; Zhang, D.; Zhang, J.; Shi, L. Enhanced Photocatalytic CO<sub>2</sub> Conversion into Reusable Fuels with Efficient Solid-State Proton Donors. *Sep. Purif. Technol.* **2025**, *354*, 129100. [\[CrossRef\]](#)
7. Vinoth Kumar, P.; Madhumitha, G. Clay Based Heterogeneous Catalysts for Carbon–Nitrogen Bond Formation: A Review. *RSC Adv.* **2024**, *14*, 4810–4834. [\[CrossRef\]](#)
8. Binhweel, F.; Ahmad, M.I.; Zaki, S.A. Utilization of Polymeric Materials toward Sustainable Biodiesel Industry: A Recent Review. *Polymers* **2022**, *14*, 3950. [\[CrossRef\]](#)
9. Karatayeva, U.; Al, A.; Narzary, B.B.; Baker, B.C.; Faul, J. Conjugated Microporous Polymers for Catalytic CO<sub>2</sub> Conversion. *Adv. Sci.* **2024**, *11*, 2308228. [\[CrossRef\]](#)
10. Carlucci, C.; Degennaro, L.; Luisi, R. Titanium Dioxide as a Catalyst in Biodiesel Production. *Catalysts* **2019**, *9*, 75. [\[CrossRef\]](#)
11. Liaquat, I.; Munir, R.; Abbasi, N.A.; Sadia, B.; Muneer, A.; Younas, F.; Sardar, M.F.; Zahid, M.; Noreen, S. Exploring Zeolite-Based Composites in Adsorption and Photocatalysis for Toxic Wastewater Treatment: Preparation, Mechanisms, and Future Perspectives. *Environ. Pollut.* **2024**, *349*, 123922. [\[CrossRef\]](#) [\[PubMed\]](#)
12. Pérez-Mayoral, E.; Matos, I.; Bernardo, M.; Ventura, M.; Fonseca, I.M. Carbon-Based Materials for the Development of Highly Dispersed Metal Catalysts: Towards Highly Performant Catalysts for Fine Chemical Synthesis. *Catalysts* **2020**, *10*, 1407. [\[CrossRef\]](#)
13. Singh, A.; Himanshu, M.; Verma, B.; Singh, R.; Lal, B.; Syed, A.; Elgorban, A.M.; Wong, L.S.; Srivastva, N. Evaluation of Sustainability of Fabrication Process and Characterization Studies of Activated Carbon Nanocatalyst from Waste Chestnut Peels. *J. Mol. Struct.* **2024**, *1321*, 139810. [\[CrossRef\]](#)
14. Kumar, S.; Soomro, S.A.; Harijan, K.; Uqaili, M.A.; Kumar, L. Advancements of Biochar-Based Catalyst for Improved Production of Biodiesel: A Comprehensive Review. *Energies* **2023**, *16*, 644. [\[CrossRef\]](#)
15. Szymański, G.S.; Karpiński, Z.; Biniak, S.; Świątkowski, A. The Effect of the Gradual Thermal Decomposition of Surface Oxygen Species on the Chemical and Catalytic Properties of Oxidized Activated Carbon. *Carbon* **2002**, *40*, 2627–2639. [\[CrossRef\]](#)
16. Reis, G.M.; Ferreira, L.; Nunes, R.S.; Mandelli, D.; Carvalho, W.A. Tailored Sulfonated Carbons: Unraveling Enhanced Catalytic Dynamics for Fructose Dehydration under Conventional and Microwave Heating. *RSC Sustain.* **2024**, *2*, 1456–1471. [\[CrossRef\]](#)
17. Almeida, K.A.; Hammer, P.; Cardoso, D. Faujasites Exchanged with Alkylammonium Cations Applied to Basic Catalysis. *Microporous Mesoporous Mater.* **2019**, *282*, 159–168. [\[CrossRef\]](#)
18. Di Serio, M.; Tesser, R.; Pengmei, L.; Santacesaria, E. Heterogeneous Catalysts for Biodiesel Production. *Energy Fuels* **2007**, *22*, 207–217. [\[CrossRef\]](#)
19. Tamborini, L.H.; Casco, M.E.; Militello, M.P.; Silvestre-Alberro, J.; Barbero, C.; Acevedo, D.F. Sulfonated Porous Carbon Catalysts for Biodiesel Production: Clear Effect of the Carbon Particle Size on the Catalyst Synthesis and Properties. *Fuel Process. Technol.* **2016**, *149*, 209–217. [\[CrossRef\]](#)
20. Nda-Umar, U.I.; Ramli, I.; Muhamad, E.N.; Azri, N.; Taufiq-Yap, Y.H. Optimization and Characterization of Mesoporous Sulfonated Carbon Catalyst and Its Application in Modeling and Optimization of Acetin Production. *Molecules* **2020**, *25*, 5221. [\[CrossRef\]](#)
21. Mateo, W.; Lei, H.; Villota, E.; Qian, M.; Zhao, Y.; Huo, E.; Zhang, Q.; Lin, X.; Wang, C.; Huang, Z. Synthesis and Characterization of Sulfonated Activated Carbon as a Catalyst for Bio-Jet Fuel Production from Biomass and Waste Plastics. *Bioresour. Technol.* **2020**, *297*, 122411. [\[CrossRef\]](#) [\[PubMed\]](#)
22. da Luz Corrêa, A.P.; Bastos, R.R.C.; da Rocha Filho, G.N.; Zamian, J.R.; da Conceição, L.R.V. Preparation of Sulfonated Carbon-Based Catalysts from Murumuru Kernel Shell and Their Performance in the Esterification Reaction. *RSC Adv.* **2020**, *10*, 20245–20256. [\[CrossRef\]](#) [\[PubMed\]](#)
23. Yang, Z.; Wang, Y.; Wu, X.; Quan, W.; Chen, Q.; Wang, A. Efficient Preparation of Biodiesel Using Sulfonated *Camellia oleifera* Shell Biochar as a Catalyst. *Molecules* **2024**, *29*, 2752. [\[CrossRef\]](#)

24. Zhu, S.; Ke, J.; Li, X.; Zheng, Z.; Guo, R.; Chen, J. Biomass Derived Sulfonated Carbon Catalysts: Efficient Catalysts for Green Chemistry. *Green Chem.* **2024**, *26*, 6361–6381. [[CrossRef](#)]
25. Migliorini, F.; Belmuso, S.; Dondè, R.; De Iulii, S.; Altman, I. To Optical Properties of Carbon Nanoparticles: A Need in Comprehending Urbach Energy. *Carbon Trends* **2022**, *8*, 100184. [[CrossRef](#)]
26. Liu, Q.; Liu, Z.; Liu, G. Solar Evaporation of Liquid Marbles with Fe<sub>3</sub>O<sub>4</sub>/CNT Hybrid Nanostructures. *J. Colloid Interface Sci.* **2025**, *677*, 25–34. [[CrossRef](#)]
27. Lagos, K.J.; Buzzá, H.H.; Bagnato, V.S.; Romero, M.P. Carbon-Based Materials in Photodynamic and Photothermal Therapies Applied to Tumor Destruction. *Int. J. Mol. Sci.* **2022**, *23*, 22. [[CrossRef](#)]
28. Shan, P.; Geng, K.; Shen, Y.; Hao, P.; Zhang, S.; Hou, J.; Lu, J.; Guo, F.; Li, C.; Shi, W. Facile Synthesis of Hierarchical Core-Shell Carbon@ZnIn<sub>2</sub>S<sub>4</sub> Composite for Boosted Photothermal-Assisted Photocatalytic H<sub>2</sub> Production. *J. Colloid Interface Sci.* **2025**, *677*, 1098–1107. [[CrossRef](#)] [[PubMed](#)]
29. Yang, Z.; Wu, Z.-Y.; Lin, Z.; Liu, T.; Ding, L.; Zhai, W.; Chen, Z.; Jiang, Y.; Li, J.; Ren, S.; et al. Optically Selective Catalyst Design with Minimized Thermal Emission for Facilitating Photothermal Catalysis. *Nat. Commun.* **2024**, *15*, 7599. [[CrossRef](#)]
30. Mehdipour-Ataei, S.; Aram, E. Mesoporous Carbon-Based Materials: A Review of Synthesis, Modification, and Applications. *Catalysts* **2023**, *13*, 2. [[CrossRef](#)]
31. Kyokunzire, P.; Zaraket, J.; Fierro, V.; Celzard, A. Recent Developments in the Use of Activated Carbon-Based Materials for Gas Sensing Applications. *J. Environ. Chem. Eng.* **2024**, *12*, 113702. [[CrossRef](#)]
32. Santamaría-Holek, I.; Hernández, S.I.; García-Alcántara, C.; Ledesma-Durán, A. Review on the Macro-Transport Processes Theory for Irregular Pores able to Perform Catalytic Reactions. *Catalysts* **2019**, *9*, 281. [[CrossRef](#)]
33. Maruyama, J.; Sumino, K.; Kawaguchi, M.; Abe, I. Influence of Activated Carbon Pore Structure on Oxygen Reduction at Catalyst Layers Supported on Rotating Disk Electrodes. *Carbon* **2004**, *42*, 3115–3121. [[CrossRef](#)]
34. Gu, X.; Qin, Y.; Wei, J.; Yuan, B.; Yu, F.; Xin, L.; Xie, C.; Yu, S. Highly Dispersed Pd Nanoparticles in Situ Reduced and Stabilized by Nitrogen-Alkali Lignin-Doped Phenolic Nanospheres and Their Application in Vanillin Hydrodeoxygenation. *Front. Chem. Sci. Eng.* **2024**, *18*, 127. [[CrossRef](#)]
35. He, C.; Duan, J.; Ma, X. Convenient Immobilization of Chiral Imidazolidinone to Hollow Polystyrene Nanospheres (HPNs) for Efficient Heterogeneous Enantioselective Friedel-Crafts Reaction. *Mol. Catal.* **2024**, *567*, 114480. [[CrossRef](#)]
36. Rai, R.K.; Gupta, K.; Tyagi, D.; Mahata, A.; Behrens, S.; Yang, X.; Xu, Q.; Pathak, B.; Singh, S.K. Access to Highly Active Ni–Pd Bimetallic Nanoparticle Catalysts for C–C Coupling Reactions. *Catal. Sci. Technol.* **2016**, *6*, 5567–5579. [[CrossRef](#)]
37. Wang, L.; Liu, X.; Jiang, Y.; Zhou, L.; Ma, L.; He, Y.; Gao, J. Biocatalytic Pickering Emulsions Stabilized by Lipase-Immobilized Carbon Nanotubes for Biodiesel Production. *Catalysts* **2018**, *8*, 587. [[CrossRef](#)]
38. Sun, Z.-P.; Zhang, X.-G.; Liang, Y.-Y.; Li, H.-L. A Facile Approach towards Sulfonate Functionalization of Multi-Walled Carbon Nanotubes as Pd Catalyst Support for Ethylene Glycol Electro-Oxidation. *J. Power Sources* **2009**, *191*, 366–370. [[CrossRef](#)]
39. Liu, C.; Yu, M.; Li, Y.; Li, J.; Wang, J.; Yu, C.; Wang, L. Synthesis of Mesoporous Carbon Nanoparticles with Large and Tunable Pore Sizes. *Nanoscale* **2015**, *7*, 11580–11590. [[CrossRef](#)]
40. Yao, Y.; Xu, J.; Huang, Y.; Zhang, T. Synthesis and Applications of Carbon Nanospheres: A Review. *Particuology* **2024**, *87*, 325–338. [[CrossRef](#)]
41. Militello, M.P.; Martínez, M.V.; Tamborini, L.; Acevedo, D.F.; Barbero, C.A. Towards Photothermal Acid Catalysts Using Eco-Sustainable Sulfonated Carbon Nanoparticles—Part I: Synthesis, Characterization and Catalytic Activity towards Fischer Esterification. *Catalysts* **2023**, *13*, 1341. [[CrossRef](#)]
42. Yusuf, B.O.; Oladepo, S.A.; Ganiyu, S.A. Efficient and Sustainable Biodiesel Production via Transesterification: Catalysts and Operating Conditions. *Catalysts* **2024**, *14*, 581. [[CrossRef](#)]
43. Wang, B.; Wang, B.; Shukla, S.K.; Wang, R. Enabling Catalysts for Biodiesel Production via Transesterification. *Catalysts* **2023**, *13*, 740. [[CrossRef](#)]
44. Shu, D.; Zhang, J.; Ruan, R.; Lei, H.; Wang, Y.; Moriko, Q.; Zou, R.; Huo, E.; Duan, D.; Gan, L.; et al. Insights into Preparation Methods and Functions of Carbon-Based Solid Acids. *Molecules* **2024**, *29*, 247. [[CrossRef](#)]
45. Tamborini, L.H.; Militello, M.P.; Balach, J.; Moyano, J.M.; Barbero, C.A.; Acevedo, D.F. Application of Sulfonated Nanoporous Carbons as Acid Catalysts for Fischer Esterification Reactions. *Arab. J. Chem.* **2019**, *12*, 3172–3182. [[CrossRef](#)]
46. Björk, E.M.; Militello, M.P.; Tamborini, L.H.; Coneo Rodríguez, R.; Planes, G.A.; Acevedo, D.F.; Moreno, M.S.; Odén, M.; Barbero, C. Mesoporous Silica and Carbon Based Catalysts for Esterification and Biodiesel Fabrication—The Effect of Matrix Surface Composition and Porosity. *Appl. Catal. A-Gen.* **2017**, *533*, 49–58. [[CrossRef](#)]
47. Netala, V.R.; Kotakadi, V.S.; Domdi, L.; Gaddam, S.A.; Bobbu, P.; Venkata, S.K.; Ghosh, S.B.; Tarte, V. Biogenic Silver Nanoparticles: Efficient and Effective Antifungal Agents. *Appl. Nanosci.* **2015**, *6*, 475–484. [[CrossRef](#)]

**Disclaimer/Publisher’s Note:** The statements, opinions and data contained in all publications are solely those of the individual author(s) and contributor(s) and not of MDPI and/or the editor(s). MDPI and/or the editor(s) disclaim responsibility for any injury to people or property resulting from any ideas, methods, instructions or products referred to in the content.